Journal for ImmunoTherapy of Cancer

NSGS mice humanized with cord blood mononuclear cells show sustained and functional myeloid–lymphoid representation with limited graft-versus-host disease

Carla Panisello ,[1,2,3] Rosario Aschero,[4] Alba Martinez-Moreno,[1,2] Heleia Roca Ho,[1,2] Aida Falgas,[1,2] Europa Azucena González-Navarro,[5,6] Julieta Carabelli,[7] Edwards Pradenas,[7] María Lázaro-Díez,[7] Julia G Prado,[3,7,8] Julià Blanco,[3,7,8,9] Jorge Carrillo,[3,7,8] Manel Juan ,[2,5,6] Ángel M Carcaboso,[4] Clara Bueno,[1,2,10] Pablo Menendez[1,2,10,11,12]

To cite: Panisello C, Aschero R, Martinez-Moreno A, *et al*. NSGS mice humanized with cord blood mononuclear cells show sustained and functional myeloid–lymphoid representation with limited graft-versus-host disease. *Journal for ImmunoTherapy of Cancer* 2024;**12**:e009198. doi:10.1136/jitc-2024-009198

► Additional supplemental material is published online only. To view, please visit the journal online (https://doi.org/10.1136/jitc-2024-009198).

Accepted 16 September 2024

For numbered affiliations see end of article.

Correspondence to
Dr Pablo Menendez; pmenendez@carrerasresearch.org

Dr Clara Bueno; cbueno@carrerasresearch.org

ABSTRACT

Humanized immunodeficient mice serve as critical models for investigating the functional interplay between transplanted human cells and a pre-reconstituted human immune system. These models facilitate the study of molecular and cellular pathogenic mechanisms and enable the evaluation of the efficacy and toxicity of immunotherapies, thereby accelerating their preclinical and clinical development. Current strategies rely on inefficient, long-term/delayed hematopoietic reconstitution by CD34+ hematopoietic progenitors or short-term reconstitution with peripheral blood mononuclear cells (PB-MNCs) associated with high rates of graft-versus-host disease (GvHD) and an inefficient representation of immune cell populations. Here, we hypothesized that immunologically naïve cord blood mononuclear cells (CB-MNCs) could serve as a superior alternative, providing long-lasting and functionally effective immune reconstitution. We conducted a comprehensive comparison between the non-obese diabetic (NOD).Cg-Prkdc^scid-IL2rg^tm1Wjl/SzJ (NSG) and NSG-Tg(CMV-IL3,CSF2,KITLG)^1Eav/MloySzJ (NSGS) immunodeficient mouse models following humanization with either PB-MNCs or CB-MNCs. We assessed the engraftment dynamics of various human immune cells over time and monitored the development of GvHD in both models. For the most promising model, we extensively evaluated immune cell functionality *in vitro* and *in vivo* using sarcoma and leukemia xenografts. Humanizing NSGS mice with CB-MNCs results in a rapid, robust, and sustained representation of a diverse range of functional human lymphoid and myeloid cell populations while minimizing GvHD incidence. In this model, human immune cell populations significantly impair the growth and engraftment of sarcoma and B-cell acute lymphoblastic leukemia cells, with a significant inverse correlation between immune cell levels and tumor growth. This study establishes a fast, efficient, and reliable *in vivo* platform for various applications in cancer immunotherapy, particularly for exploring the complex interactions between cancer cells, immune cells, and the tumor microenvironment *in vivo*, prior to clinical development.

INTRODUCTION

Humanized immunodeficient mouse models offer significant potential for accelerating preclinical research and clinical development of novel therapies. By establishing or reconstituting a functional human immune system in these models, the complex interactions between human cancer cells, immune cells and the tumor microenvironment (TME) can be studied *in vivo*. These models are invaluable for dissecting the molecular and cellular mechanisms underlying specific diseases and for driving the development of novel therapeutic strategies.[1] Recent advances in cellular immunotherapies have relied heavily on insights gained from humanized mouse models, particularly in elucidating the mechanisms underlying immune checkpoint inhibition, CAR-T cell therapies and monoclonal antibody-based therapies.[2–6] Evaluating the efficacy and safety of these immunotherapeutic strategies in a setting that closely mimics the human immune system is critical and expedites their clinical translation.[2 7]

Historically, humanization efforts have used two main approaches: (1) engraftment of immunodeficient mice with CD34+ hematopoietic stem and progenitor cells (HSPCs) from cord blood (CB), bone marrow (BM) or fetal liver (FL) or (2) the use of peripheral blood mononuclear cells (PB-MNCs).[8] While these approaches have made significant contributions to the field, they each present

unique challenges. CD34+HSPCs offer hematopoietic engraftment potential, but with limited representation of lymphoid and myeloid cell types and can take longer than 20 weeks.[9 10]PB-MNC humanization, although faster, is associated with high levels of graft-versus-host disease (GvHD) and associated mortality, and often lacks diverse lymphoid–myeloid representation.[1]The inherent limitations of current humanization strategies underscore the need for novel models that achieve a balance between rapid and sustained engraftment, minimized GvHD, and diverse human immune reconstitution. In addition, the immunodeficient mouse strain used may influence the efficiency and persistence of the humanized graft. The most common immunodeficient mouse strains used in humanization strategies are Rag2−/− mice, severe combined immunodeficient mice and non-obese diabetic. Cg-Prkdc scid IL2rg tm1Wjl/SzJ (NSG) mice.

To address these challenges, we aimed to use cord blood mononuclear cells (CB-MNCs) as an alternative immunologically naïve source for humanization in NSG and NSG-Tg(CMV-IL3,CSF2,KITLG)1Eav/MloySzJ (NSGS) mice which express human interleukin-3 (IL-3), granulocyte-macrophage colony-stimulating factor (GM-CSF) and stem cell factor.[11] The study presents a comprehensive comparison between humanization using CB-MNCs and conventional PB-MNCs protocols, focusing on the incidence of GvHD, human engraftment kinetics, and the reconstitution dynamics of various human immune cell populations. We evaluated the functionality of the transplanted human immune cells both *ex vivo* and *in vivo*. The CB-MNC-humanized NSGS model exhibited rapid, sustained, and functional myeloid-lymphoid engraftment with a low risk of GvHD. These findings establish this model as an efficient and reliable platform for a wide range of applications in cancer immunotherapy studies, particularly in investigating the complex interactions between cancer cells, immune cells, and the TME.

MATERIALS AND METHODS

Sourcing and processing of CB-MNCs and PB-MNCs

B-cell acute lymphoblastic leukemia (B-ALL) blasts and PB- and CB-MNCs were isolated from gender-balanced individuals by Ficoll-Hypaque gradient centrifugation.[12] B-ALL samples, buffy coats (n=3) and CBs (n=3) were obtained from the collaborating hospitals and the Catalan Blood and Tissue Bank, respectively.

Humanization of NSG and NSGS mice and flow cytometry assessment

Seven-to-ten-week-old NSG and NSGS mice were obtained from Charles River Laboratories (Wilmington, Massachusetts, USA) and The Jackson Laboratory respectively (Bar Harbor, Maine, USA) and were bred and housed under pathogen-free conditions. A total of 5×10^6 PB-MNCs or CB-MNCs were transplanted intravenously into sublethally irradiated (2 Gy) mice.[6] To prevent potential variabilities due to sex of the mice, a total of 39 mice were used, comprising 19 females and 20 males. Human cell engraftment and assessment of immune cell populations were monitored weekly in PB by flow cytometry. Animals showing GvHD clinical signs, such as weight and hair loss, antalgic posture, and decreased activity, were euthanized.[13 14] PB, BM, liver and spleen were harvested for immunophenotyping. The emergence of GvHD signs was evaluated as event-free survival (EFS).

HLA-ABC-PE (G46-2.6, BD-Pharmingen) and CD45-PerCP-Cy5.5 (2D1, BD-Biosciences) antibodies were used to identify human immune-hematopoietic grafts (HLA-ABC+CD45+ population) weekly in PB and at endpoint from BM, liver and spleen. For immunophenotyping of immune cell subsets within the human graft, CD19-APC-H7 (SJ25C1, BD-Pharmingen), CD3-PECy7 (UCHT1, BD-Pharmingen), CD4-BV421 (RPA-T4, BD-Horizon), CD8-BV510 (SK1, BD-Horizon), CD7-FITC (B M-T701, BD-Pharmingen) and CD33-APC (WM53, BD-Pharmingen) antibodies were used to identify B cells (CD19+), CD4+ (CD3+CD4+) or CD8+ (CD3+CD8+) T cells, NK cells (CD3-CD7+)[15–17] and monocytes (CD33+) by flow cytometry on a FACSCanto-II cytometer running FACSDiva software (BD-Biosciences). Before the infusion of mononuclear cells (MNCs), the differentiation status of T cells was determined using CD3-PECy7, CCR7-PE (3D12, BD-Pharmingen), CD45RA-BV510 (HI100, BD-Horizon) and CD95-APC (DX2, BD-Pharmingen) antibodies. This combination allowed the identification of naïve (N, CCR7+CD45RA+CD95−), stem cell memory (SCM, CCR7+CD45RA+CD95+), central memory (CM, CCR7+CD45RA−), effector memory (EM, CCR7-CD45RA−) and terminally differentiated EM cells re-expressing CD45RA (EMRA, CCR7-CD45RA+) T cells.[13]

Ex vivo functional assessment of the immune cell types in CB-MNC-humanized NSGS mice

NSGS mice humanized with CB-MNCs were euthanized 8 weeks following transplantation, after achieving a human graft >20%. Single-cell suspensions were obtained from PB, BM, liver and spleen and used to assess *ex vivo* the functionality of B cells, CD4+and CD8+ T cells, NK cells and monocytes on cell type-specific activation. A total of 1×10^6 cells/mL were seeded in a 48-well plate in RPMI-1640 medium supplemented with 10% fetal bovine serum, 1% penicillin/streptomycin and 1% GlutaMAX (Gibco/Life Technologies). For assessment of B-cell activation, the expression of CD86-FITC (2331, BD-Biosciences) and CD69-BV510 (FN50, BioLegend) was analyzed on B cells after stimulation for 3 days with 50 ng/mL CD40L-HA tagged (6420-CL, R&DSystems), 1 µg/mL anti-HA-Tag antibody (12CA5, Roche) and 10 ng/mL IL-4 (AF-200-04, PeproTech).[18] Activation of human BM CD4+ and CD8+ T cells and NK cells was determined by staining with CD25-APC-Cy7 (BC96, BioLegend), interferon (IFN) γ-PECy7 (4S.B3, BioLegend) and CD107a-PerCP-Cy5.5 (H4A3, BioLegend)[19] on stimulation with 25 ng/mL phorbol-12-miristate-13-acetate (PMA) (P1585, Sigma-Aldric) and 1 µg/mL ionomycin (I0634, Sigma-Aldrich)

for 4 hours. Human PB monocytes were stimulated with 10 ng/mL lipopolysaccharide (LPS) (L2630, Sigma-Aldrich) for 6 hours and activation was assessed by CD69-BV510 and tumor necrosis factor (TNF)α-PE-Cy7 (MAb11, BioLegend) expression.[20 21] The GolgiPlug reagent (555029, BD-Biosciences) was added for intracellular analysis of IFNγ and TNFα 30 min before stimulation. All experiments were replicated using at least three CB samples from different donors.

Assessment of tumor engraftment in CB-MNC-humanized NSGS mice

NSGS mice humanized with CB-MNCs were transplanted subcutaneously (s.c.) with 1×10^6 A673 Ewing sarcoma cells (ATCC). Non-humanized NSGS mice were used as controls for A673 tumor growth. Human immune cell levels in mice were assessed using the humanization antibody panel described above prior to transplantation. Murine PB was then monitored weekly by flow cytometry to follow the CB-MNC-derived immune cell populations. Subcutaneous tumor volume (mm^3) was quantified as $(length\times width^2)/2$ using a caliper. Animals were euthanized 4 weeks after A673 transplantation and human immune cell engraftment was assessed in PB, BM, liver, spleen as well as within the tumor at endpoint. A portion of the engrafted tumor was harvested for immunofluorescence to assess the presence of tumor-infiltrating human immune cells. To further characterized tumor engraftment in CB-MNC-humanized NSGS mice, an aggressive B-ALL PDX model was used. CB-MNC-humanized NSGS mice were transplanted with 1×10^6 B-ALL cells, and the B-ALL engraftment was assessed weekly in PB. Three weeks post-transplantation, the animals were euthanized, and human immune cell engraftment was evaluated in PB, BM, liver and spleen. All experiments were replicated using at least three CB samples from different donors.

HLA-typing of A673 cells, B-ALL PDX cells and CB-MNCs

HLA class I (A, B, C) and class II (DRB1, DQB1, DPB1) typing was performed using DNA next-generation sequencing.[22] Online supplemental table S1 shows the HLA matching loci between the A673 cell line, B-ALL cells, and CB-MNCs. Genomic DNA from CB-MNCs and B-ALL samples was extracted Maxwell RSC Blood DNA protocol (AS1400, Promega).

Immunofluorescence analysis of immune populations in the subcutaneous tumor

Tumors were embedded in Tissue-Tek OCT compound (4538, Sakura) and sectioned at a thickness of 6 µm. The sections were fixed with 4% paraformaldehyde for 20 min, permeated with 0.1% Triton X-100 (T8787, Sigma-Aldrich) and blocked for 30 min with 1% BSA (A4503, Sigma-Aldrich). Primary antibodies CD99 (NCL-L-CD99-187, Leica) and CD45 (LCA-L-CE, Leica) were incubated overnight at 4°C, followed by incubation with a secondary antibody (A32744, Invitrogen) for 1 hour at room temperature. DAPI (62248,Thermo Fisher) was added for nuclear staining, and sections were mounted with Vectashield (H-1000-10, Vector Laboratories).

Statistical analyses

In all humanization experiments, each dot represents one independent mouse. The remaining data are represented as the mean±SE of mean. A two-tailed paired t-test was used to compare the secretion and expression levels of markers in unstimulated and stimulated cells. Pearson test was used for correlation analyses. All p values were two tailed and statistical significance was defined as *p<0.05, **p<0.01, ***p<0.001, ****p<0.0001. All analyses were performed with Prism software V.8.0 (GraphPad Prism).

RESULTS

Limited GvHD and sustained myeloid–lymphoid representation in NSGS mice transplanted with CB-MNCs

Humanization of immunodeficient mice with PB-MNCs often leads to high rates of GvHD, increased mortality, and an imbalance in human immune cell representation. However, the humanization of these mice with more immunologically naïve CB-MNCs has not been thoroughly characterized. Here, we prospectively compare the incidence of GvHD, total human engraftment, and the representation of human immune cell subsets in NSG and NSGS mice humanized with either PB-MNCs or CB-MNCs from three different donors over 13 weeks (Figure 1A,B). Prior to humanization, the immune cell composition of PB-MNCs and CB-MNCs was analyzed, revealing only slight differences in the monocyte and B cell populations between both MNCs sources (Figure 1C).

Both NSG and NSGS mice humanized with PB-MNCs exhibited signs of GvHD as early as 2 weeks post-transplantation, and by 8 weeks, over 70% of the mice displayed severe disease symptoms (Figure 1D). Immune engraftment analysis revealed that approximately 80% of the mice achieved >20% engraftment at 2 weeks (Figure 1E). However, this engraftment lacked balanced representation of myeloid-lymphoid immune cell subsets, being dominated by CD4+ and CD8+ T cells (Figure 1F), which likely contributed to the early onset of GvHD. Conversely, transplantation with CB-MNCs resulted in very low levels of GvHD at 8 weeks, with 80% EFS observed across both mouse strains (Figure 1G). Human engraftment kinetics were slower in mice humanized with CB-MNCs compared with those with PB-MNCs, but engraftment levels were significantly higher in NSGS mice than in NSG mice. In NSGS mice, human engraftment reached and maintained levels of 18%–30% between weeks 7 and 13 (Figure 1H). Notably, analysis of immune cell subsets revealed a balanced myeloid–lymphoid reconstitution in mice humanized with CB-MNCs, consisting of B cells, CD4+ and CD8+ T cells, NK cells and monocytes from week 7 (Figure 1I). In NSGS mice, engraftment of human NK cells and monocytes was higher than in NSG, and sustained until the endpoint (Figure 1I). To further assess the robustness of humanization with CB-MNCs,

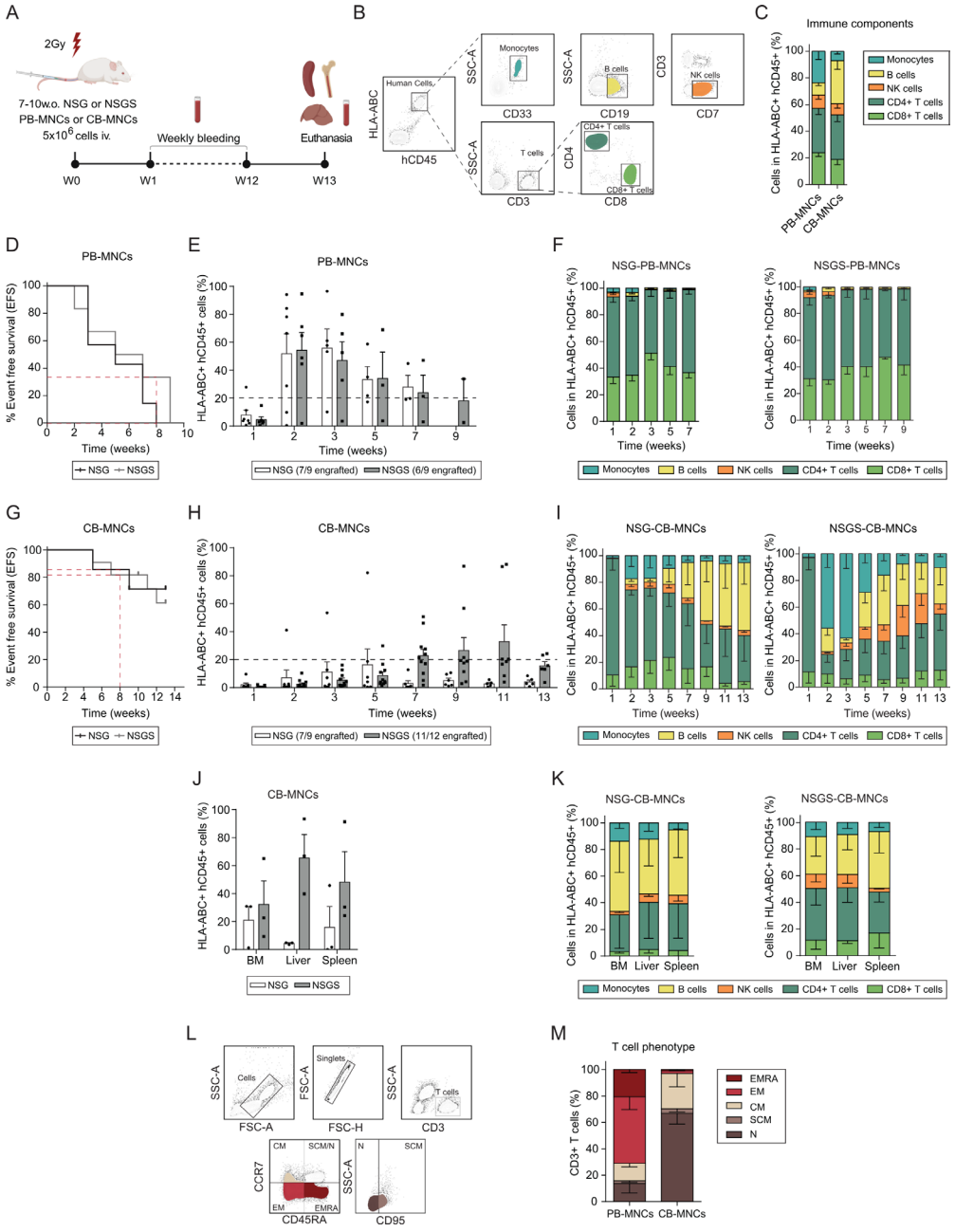

Figure 1 NSGS mice humanized with CB-MNCs show a rapid and sustained myeloid–lymphoid representation and low GvHD rates. (A) Schematic representation of the experimental design used to evaluate different humanization models. (B) Flow cytometry gating strategy employed to identify human immune cell subsets in mouse hematopoietic tissues. (C) PB and CB immune cell populations before MNC infusion in NSG and NSGS mice. (D) Kaplan-Meier event-free survival (EFS) curve over 10 weeks for NSG (n=9) and NSGS (n=9) mice transplanted with PB-MNCs. (E) Percentage of human immune cell (HLA-ABC+hCD45+) engraftment in the PB of NSG (n=9) and NSGS (n=9) mice transplanted with PB-MNCs monitored over a 9-week period. (F) Proportion of different human immune cell subsets within the HLA+hCD45+ human graft in the PB of NSG (n=9) and NSGS (n=9) mice transplanted with PB-MNCs. (G) Kaplan-Meier EFS over 14 weeks for NSG (n=9) and NSGS (n=12) mice transplanted with CB-MNCs. (H) Percentage of HLA-ABC+hCD45+ engraftment in the PB of NSG (n=9) and NSGS (n=9) mice transplanted with CB-MNCs monitored over a 13-week period. (I) Proportion of different human immune cell subsets within the HLA+hCD45+ human graft in the PB of NSG (n=9) and NSGS (n=12) mice transplanted with CB-MNCs. (J) Total engraftment of HLA-ABC+hCD45+ in BM, liver and spleen of NSG (n=3) and NSGS (n=3) mice transplanted with CB-MNCs. (K) Proportion of different human immune cell subsets within the HLA-ABC+hCD45+ population in BM, liver and spleen at the endpoint in NSG (n=3) and NSGS (n=3) mice transplanted with CB-MNCs. (L) Flow cytometry gating strategy used to study the T cell phenotype before PB-MNC or CB-MNC transplantation. (M) PB (n=3) and CB (n=3) T cell phenotype before transplantation. Combined results from NSGS mice humanized with PB or CB samples from three different donors are shown. Each dot represents an independent mouse. CB-MNCs, cord blood mononuclear cells; CM, central memory; EM, effector memory; EMRA, terminally differentiated effector memory cells re-expressing CD45RA; GvHD, graft-versus-host disease; N, naïve; PB-MNCs, peripheral blood mononuclear cells; SCM, stem cell memory.

we analyzed other hematopoietic organs including BM, liver and spleen. We confirmed superior engraftment in all these tissues in NSGS mice (Figure 1J), with a similar representation of the different immune cell subsets across both mouse strains (Figure 1K).

To understand why mice humanized with CB-MNCs take longer to engraft and exhibit less GvHD in both mouse strains, we analyzed the T-cell phenotype in PB-MNCs and CB-MNCs before infusion. The results showed that, unlike PB-derived T cells, CB-derived T cells mostly exhibited a naïve phenotype(CCR7+CD45RA+CD95–; 66.95%±8.25% vs 13.77%±7.23%, p<0.05). This naïve phenotype is less capable of recognizing mouse structures, thereby leading to a reduced incidence of GvHD (Figure 1L,M).

Human immune cells in NSGS mice humanized with CB-MNCs are functional *ex vivo*

Next, we aimed to determine whether the different myeloid and lymphoid CB-MNC subsets expanded in NSGS mice were functional. To test this, CB-MNCs were transplanted into NSGS mice, and at week 7—when >20% total PB engraftment was observed, and all immune cell types were represented across organs—the mice were euthanized. Immune cells were then harvested and exposed to specific stimuli *ex vivo* (Figure 2A–C). Spleen-derived cells were stimulated with CD40L and IL-4 to promote B-cell activation. After 3 days, CD69 and CD80 expression was significantly higher in stimulated B cells compared with unstimulated cells (Figure 2D). BM-derived cells were stimulated with PMA and ionomycin for 4 hours to activate CD4+ and CD8+ T cells, as well as NK cells. Analysis of IFNγ secretion revealed significantly higher levels in all three cell types following stimulation (Figure 2E–G). Additionally, CD25 was overexpressed in both CD4+ and CD8+ T cells after PMA/ionomycin stimulation (Figure 2E,F). To further assess the functionality of CD8+T cells and NK cells, we evaluated degranulation levels and observed significantly higher CD107a expression in stimulated CD8+T cells and NK cells compared with unstimulated cells (Figure 2F,G). Finally, PB cells were LPS-stimulated to induce monocyte activation, resulting in a significant increase in TNFα secretion and CD69 expression after 6 hours (Figure 2H), confirming their functionality.

Human immune cells in CB-MNC-humanized NSGS mice infiltrate xenotransplanted solid tumors and correlate with lower tumor growth

We then assessed the feasibility of solid tumor engraftment by s.c. injecting A673 Ewing sarcoma cells into NSGS mice that had been humanized 6 weeks prior with variable HLA haplotype CB-MNCs from three different donors (online supplemental table S1). Non-humanized NSGS mice served as controls for A673 tumor growth. Tumor growth and humanization status were monitored weekly, and mice were euthanized 4 weeks post-transplantation. Hematopoietic organs and tumors were then harvested for immune cell population analysis (Figure 3A). After 4 weeks, overall survival was significantly higher in humanized mice compared with non-humanized controls (Figure 3B). However, despite the presence of human immune cells, ~90% of the humanized mice developed tumors after 4 weeks, with variable growth kinetics and tumor weights (Figure 3C,D), regardless of the HLA haplotype of the CB-MNC sample. Human immune cell infiltration was examined in PB, BM, liver, spleen, and within the s.c. engrafted tumors. The analysis revealed higher immune cell infiltration in all hematopoietic organs compared with the tumors, where the immune infiltrate ranged from 0.5% to 2% (Figure 3E,F). The distribution of immune cells in the A673 Ewing sarcoma tumors largely differed from that in hematopoietic organs, with monocytes being the most prominently represented cell type. T cells were notably sparse within the tumors (Figure 3G).

A673 tumor growth and human immune infiltrate varied among mice, suggesting an association between the presence of human immune cells and tumor growth. To explore this, we correlated immune cell populations in PB at the endpoint with Ewing sarcoma tumor volume. Our analysis revealed that higher human immune infiltration was significantly associated with reduced Ewing sarcoma volume particularly due to the presence of B cells, NK cells, and T cells (Figure 3H–L). Additionally, we studied the behavior of a B-ALL PDX with an aggressive systemic engraftment in this humanized model (online supplemental figure S1A–C). Consistent with the Ewing sarcoma model, we found that leukemia engraftment at the endpoint of the study was also significantly lower in humanized mice (online supplemental figure S1D). Infiltration of human NK cells and T cells also showed a significant correlation with reduced leukemia multiorgan engraftment in PB, BM, liver, and spleen (online supplemental figure S1E).

DISCUSSION

Current murine humanization models using PB-MNCs or CD34+HSPCs derived from CB, BM or FL have significant limitations.[7 8 23] A drawback of PB-MNC humanization is the high risk of GvHD and an incomplete representation of the immune system in the mice. By contrast, CD34+HSPC humanization is temporally limited, as mice require 20–24 weeks to achieve humanization.[9] In this study, we showed a balanced and sustained reconstruction of the immune system, including B cells, CD4+and CD8+ T cells, NK cells, and monocytes, starting from week 7 in NSGS mice infused with CB-MNCs. These populations, particularly B cells, NK cells and monocytes, were minimally found in the PB-MNC model. Furthermore, we found a higher number of immature/naïve T cells in CB-MNCs than in PB-MNCs, which would explain the low levels of GvHD found in this model. Collectively, CB-MNCs demonstrate advantages over PB-MNCs in terms of reduced GvHD and sustained, balanced representation of myeloid–lymphoid

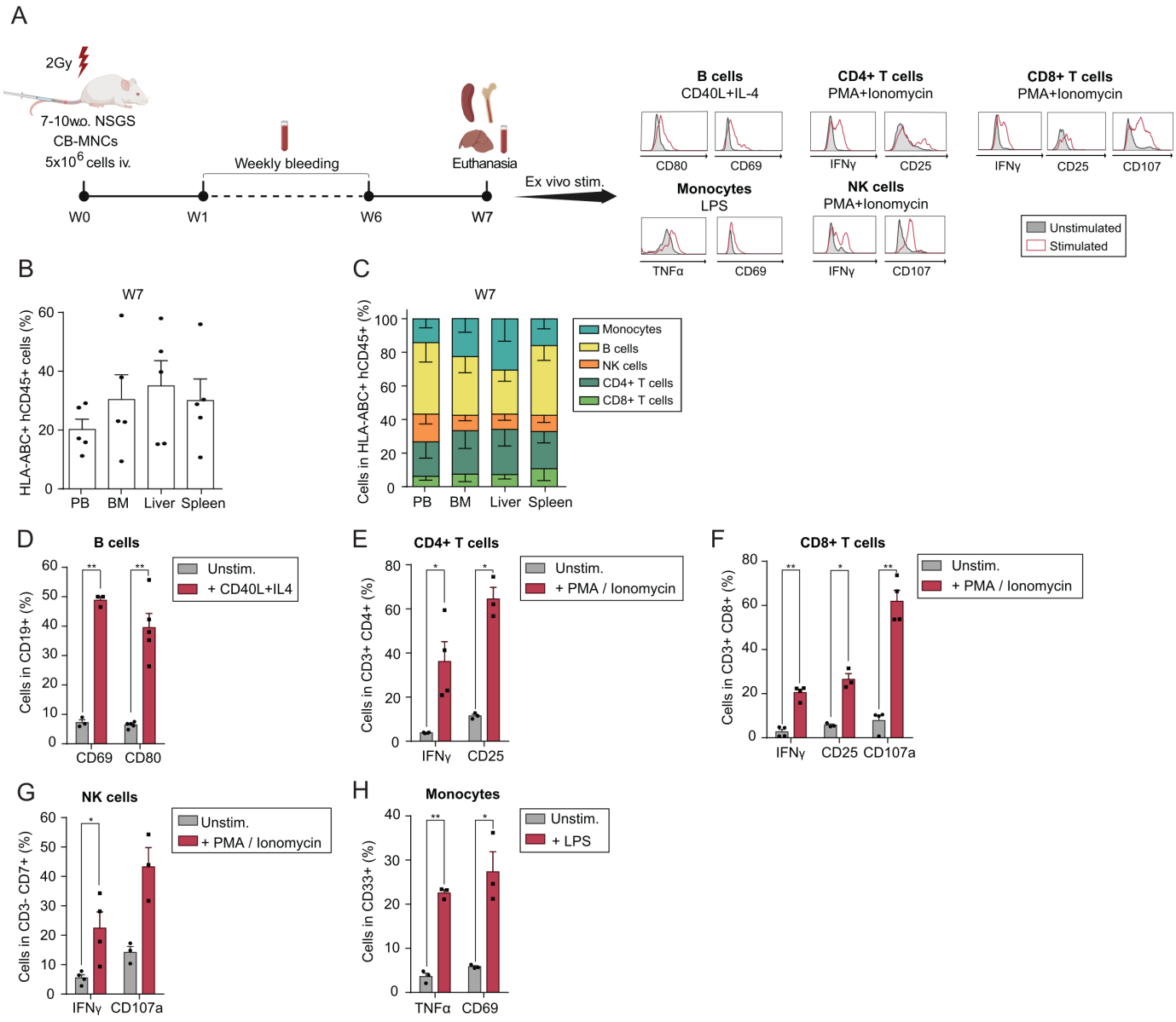

Figure 2 Expansion of functional human immune cell populations in NSGS Mice Humanized with CB-MNCs. (A) Schematic overview of the experimental design employed to assess the *ex vivo* functionality of human immune cells isolated from humanized NSGS mice. Representative flow cytometry plots are shown, depicting the activation status of human immune cell populations. (B, C) Engraftment of total HLA-ABC+hCD45+ (B) and the proportion of immune populations within the HLA+hCD45+ human graft (C) before *ex vivo* stimulation (week 7) in PB, BM, liver, and spleen from NSGS mice transplanted with CB-MNCs. (D) Expression of CD69 and CD80 activation markers in B cells *ex vivo*-stimulated with CD40L and IL-4. (E) Frequency of IFNγ- and CD25-expressing CD4+T cells after *ex vivo* stimulation with PMA and ionomycin. (F) Frequency of IFNγ, CD25, and CD107a-expressing CD8+T cells after *ex vivo* stimulation with PMA and ionomycin. (G) Expression of IFNγ and CD107a in NK cells after *ex vivo* stimulation with PMA and ionomycin. (H) Proportion of TNFα+ and CD69+ monocytes after *ex vivo* stimulation with LPS. Three independent donors were used. Each dot represents data from an independent mouse. *p<0.05, **p<0.01, paired t-test. BM, bone marrow CB-MNCs, cord blood mononuclear cells; LPS, lipopolysaccharide; PB, peripheral blood; PMA, phorbol-12-miristate-13-acetate.

immune cell subsets in primary and secondary hematopoietic organs, especially in NSGS mice.

The functionality of the engrafted CB-derived human immune cells, including increased activation markers, cytokine secretion, and T and NK cell degranulation, was validated *ex vivo*. The *in vivo* functional implication of this model was assessed using an Ewing sarcoma xenograft model in NSGS mice that had been humanized with CB-MNCs from different donors CB-MNCs. Despite having a competent humanized immune system, solid tumors developed in most mice. However, the presence of human immune cells lowered tumor growth, further demonstrating the potential of this system in cancer. Similar data were also observed on inoculation of an aggressive B-ALL PDX in NSGS mice that had been humanized with CB-MNCs. Interestingly, immune

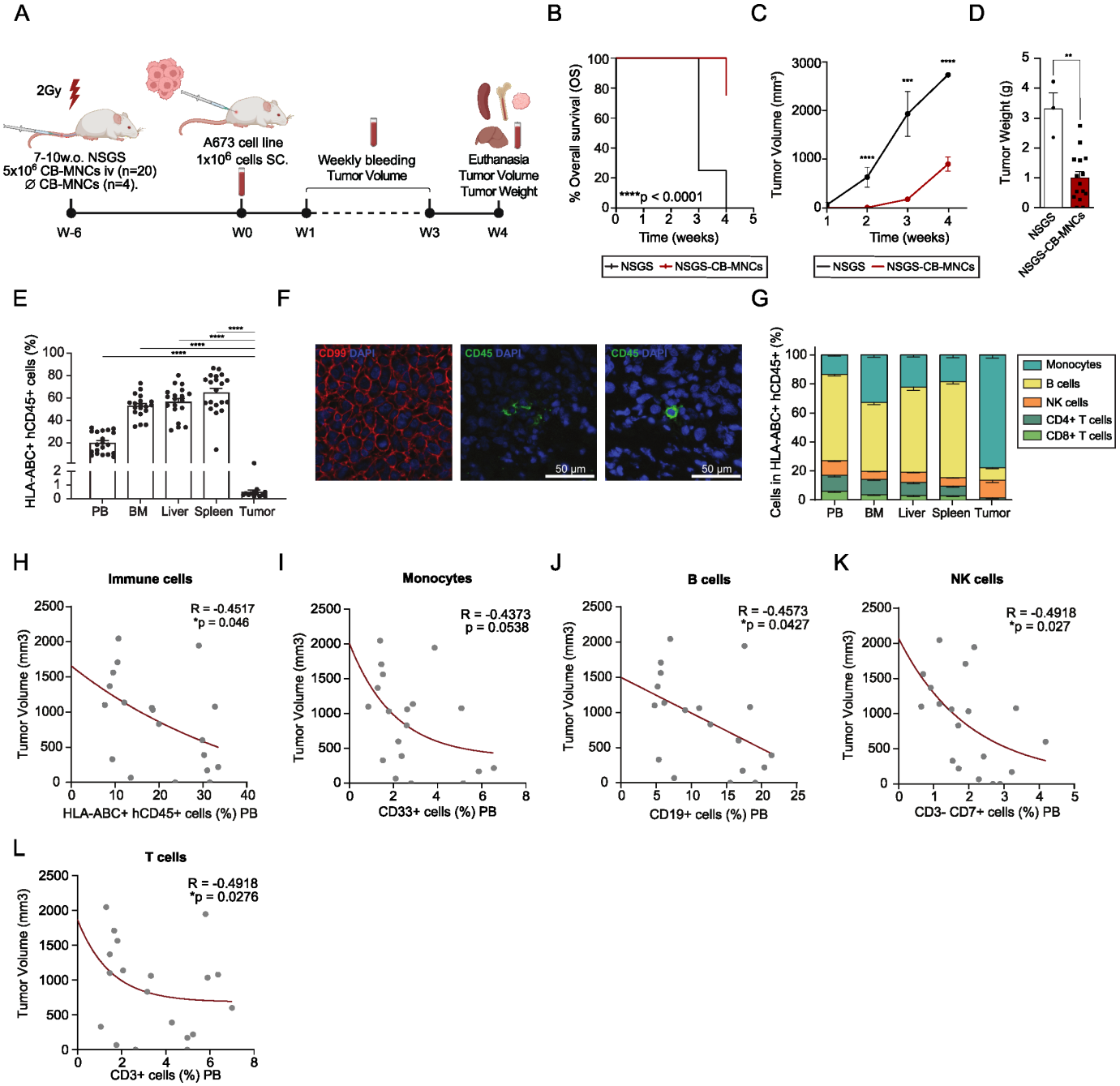

Figure 3 Human immune cell populations infiltrate subcutaneously engrafted tumors and delay tumor growth in NSGS mice humanized with CB-MNCs. (A) Schematic representation of the experimental design used to assess the tumor immunity of human immune cells against ES *in vivo*. (B) Kaplan-Meier overall survival (OS) curve for CB-MNCs humanized (n=20) and non-humanized (n=4) NSGS mice subcutaneously transplanted with A673 cells. (C) Weekly monitoring of tumor volume (mm^3) after A673 transplantation. (D) Tumor weight (g) of independent mice at endpoint. (E) Total HLA-ABC+hCD45+ engraftment at endpoint in PB, BM, liver, spleen and subcutaneously engrafted tumors (tumor infiltration) from NSGS mice transplanted with CB-MNCs. (F) Representative immunofluorescence image of CD99+tumor cells (red) and tumor-infiltrating human CD45+immune cells (green). (G) Proportion of immune populations within the HLA+hCD45+ human graft identified at endpoint in PB, BM, liver, spleen and in subcutaneously engrafted tumors (tumor infiltration) from NSGS mice transplanted with CB-MNCs. (H–L) Correlation of tumor volume (mm^3) with HLA-ABC+hCD45+ (H), Monocytes (I), B cells (J), NK cells (K) and T cells (L) in mouse PB at endpoint. Three independent donors were used. Each dot represents an independent mouse. *p<0.05, **p<0.01, ***p<0.001, ****p<0.0001, Pearson correlation test. BM, bone marrow; CB-MNCs, cord blood mononuclear cells; PB, peripheral blood.

cell infiltration with a low representation of T cells was observed on the solid tumor site, mimicking the architecture of a cold-TME present in Ewing sarcoma and other tumors.[24 25] This *in vivo* functionality and tumor infiltrating capacity of CB-MNCs prompts its application to study the *in vivo* interaction between immune cells,

cancer cells and the TME and may serve as a platform for assessing cancer immunotherapies.

Despite the advantages of using CB-MNCs for humanization, there are notable limitations to our model. First, the use of CB-MNCs, which are not patient-specific, can affect the model's ability to fully replicate human tumor biology and immune responses. This allogeneic system may not accurately mimic individual patient conditions. Additionally, controlling immune engraftment levels in individual mice presents a challenge, leading to some degree of intermouse variability which may eventually impact the consistency of results. Finally, our study is restricted to used two tumor models, sarcoma and leukemia. While the model shows promise for studying immunotherapies and tumor-immune system interactions further research should expand to include a broader range of epithelial cancer types.

Collectively, NSGS mice humanized with CB-MNCs serve as an efficient and reliable platform for studying the infiltration and interaction of functional human myeloid–lymphoid cells in xenografted human tumors. This model opens new avenues for assessing novel immunotherapies.

Author affiliations
[1]Josep Carreras Leukaemia Research Institute (IJC), Barcelona, Spain
[2]Red Española de Terapias Avanzadas (TERAV), Instituto de Salud Carlos III (ISCIII), Madrid, Spain
[3]Germans Trias i Pujol Research Institute (IGTP), Badalona, Spain
[4]Paediatric Cancer Treatment, Sant Joan de Deu Research Institute, Barcelona, Spain
[5]Department of Immunology and Immunotherapy, Hospital Clínic Barcelona, Barcelona, Spain
[6]August Pi i Sunyer Institute of Biomedical Research (IDIBAPS), Barcelona, Spain
[7]IrsiCaixa AIDS Research Institute, Badalona, Spain
[8]Centro de Investigación Biomédica en Red en Enfermedades Infecciosas (CIBERINFEC), Instituto de Salud Carlos III (ISCIII), Madrid, Spain
[9]Department of Microbiology, Universitat Autònoma de Barcelona, Bellaterra, Spain
[10]Centro Investigación Biomédica en Red en Oncología (CIBERONC), Instituto de Salud Carlos III (ISCIII), Madrid, Spain
[11]Institució Catalana de Recerca i Estudis Avançats (ICREA), Barcelona, Spain
[12]Departament of Biomedicine, School of Medicine, Universitat de Barcelona, Barcelona, Spain

X Clara Bueno @clarabueno74

Acknowledgements The authors extend their sincere thanks to Dr Patricia Pérez-Galán, Dr Ferran Araujo-Ayala, Dr María Velasco, Dr Ángel Luís Corbí, and Dr Enrique de Álava for their invaluable technical support and insightful suggestions. Artwork was generated using BioRender.

Contributors CP, RA, AM-M, HRH, AF, EAG-N, JCarabelli, EP, and ML-D performed experiments and interpreted data. JGP, JB, JCarrillo, MJ, AMC, CB and PM supervised research and contributed key knowledge, techniques, and reagents. CP, CB and PM conceived the study and funded the research. All authors have read and agreed to publish the manuscript.

Funding This research has been made possible through funding provided by the "la Caixa" Foundation (CaixaImpulse Grant CI21-00189), the Spanish Ministry of Economy and Competitiveness, and the European Union under the "NextGenerationEU/PRTR" (PLEC2022-009416, MCIN/AEI/10.13039/501100011033/) and the European Research Council (ERC) PoC Grant (BiTE-CAR, 101100665). Additional support was received from the "Ayudas Merck de Investigación" granted by Fundación Merck and H2020 EU funding (101057250-CANCERNA). The PM lab also acknowledges support from ISCIII-RICORS TERAV within the Next Generation EU program (Plan de Recuperación, Transformación y Resilencia). Core support in the PM laboratory is provided by CERCA/Generalitat de Catalunya and Fundació Josep Carreras-Obra Social la Caixa. CP was supported by the PFIS fellowship from ISCIII (FI21/00161). AF was supported by a Juan de la Cierva postdoctoral fellowship (FJC2021-046789-I).

Competing interests PM is founder of the spin-off OneChain Immunotherapeutics, which has no connection with the present research. The remaining authors declare no competing interests.

Patient consent for publication Not applicable.

Ethics approval This study involves human participants and was approved by the institutional review board, Barcelona Clinic Hospital Ethics Committee (ID: HCB/2023/0124). Buffy coats and cord blood were obtained from the Barcelona Blood and Tissue Bank after institutional review board approval by Barcelona Clinic Hospital Ethics Committee (ID: HCB/2018/0030). Participants gave informed consent to participate in the study before taking part. All in vivo procedures were approved by the institutional review board, Animal Care Committee of the Barcelona Biomedical Research Park (DAAM11833).

Provenance and peer review Not commissioned; externally peer reviewed.

Data availability statement All data relevant to the study are included in the article or uploaded as online supplemental information. All data relevant to the study are included in the article. The raw data generated in this study are available on reasonable request to the corresponding author.

ORCID iDs
Carla Panisello http://orcid.org/0000-0002-8437-4418
Manel Juan http://orcid.org/0000-0002-3064-1648

REFERENCES

1 Allen TM, Brehm MA, Bridges S, *et al*. Humanized immune system mouse models: progress, challenges and opportunities. *Nat Immunol* 2019;20:770–4.
2 Chuprin J, Buettner H, Seedhom MO, *et al*. Humanized mouse models for immuno-oncology research. *Nat Rev Clin Oncol* 2023;20:192–206.
3 Capasso A, Lang J, Pitts TM, *et al*. Characterization of immune responses to anti-PD-1 mono and combination immunotherapy in hematopoietic humanized mice implanted with tumor xenografts. *J Immunother Cancer* 2019;7:37.
4 Hu X, Manner K, DeJesus R, *et al*. Hypoimmune anti-CD19 chimeric antigen receptor T cells provide lasting tumor control in fully immunocompetent allogeneic humanized mice. *Nat Commun* 2023;14:2020.
5 Norelli M, Camisa B, Barbiera G, *et al*. Monocyte-derived IL-1 and IL-6 are differentially required for cytokine-release syndrome and neurotoxicity due to CAR T cells. *Nat Med* 2018;24:739–48.
6 Rius Ruiz I, Vicario R, Morancho B, *et al*. p95HER2-T cell bispecific antibody for breast cancer treatment. *Sci Transl Med* 2018;10:eaat1445.
7 Cogels MM, Rouas R, Ghanem GE, *et al*. Humanized Mice as a Valuable Pre-Clinical Model for Cancer Immunotherapy Research. *Front Oncol* 2021;11:784947.
8 Verma B, Wesa A. Establishment of Humanized Mice from Peripheral Blood Mononuclear Cells or Cord Blood CD34+ Hematopoietic Stem Cells for Immune-Oncology Studies Evaluating New Therapeutic Agents. *Curr Protoc Pharmacol* 2020;89:e77.
9 Park N, Pandey K, Chang SK, *et al*. Preclinical platform for long-term evaluation of immuno-oncology drugs using hCD34+ humanized mouse model. *J Immunother Cancer* 2020;8:e001513.

10 O'Brien LJ, Walpole CM, Leal-Rojas IM, *et al*. Characterization of Human Engraftment and Hemophagocytic Lymphohistiocytosis in NSG-SGM3 Neonate Mice Engrafted with Purified CD34^{+} Hematopoietic Stem Cells. *Exp Hematol* 2024;130:104134.
11 Wunderlich M, Chou F-S, Sexton C, *et al*. Improved multilineage human hematopoietic reconstitution and function in NSGS mice. *PLoS One* 2018;13:e0209034.
12 Baroni ML, Sanchez Martinez D, Gutierrez Aguera F, *et al*. 41BB-based and CD28-based CD123-redirected T-cells ablate human normal hematopoiesis in vivo. *J Immunother Cancer* 2020;8:e000845.
13 Blanco B, Ramírez-Fernández Á, Bueno C, *et al*. Overcoming CAR-Mediated CD19 Downmodulation and Leukemia Relapse with T Lymphocytes Secreting Anti-CD19 T-cell Engagers. *Cancer Immunol Res* 2022;10:498–511.
14 Naserian S, Leclerc M, Thiolat A, *et al*. Simple, Reproducible, and Efficient Clinical Grading System for Murine Models of Acute Graft-versus-Host Disease. *Front Immunol* 2018;9:10.
15 Milush JM, Long BR, Snyder-Cappione JE, *et al*. Functionally distinct subsets of human NK cells and monocyte/DC-like cells identified by coexpression of CD56, CD7, and CD4. *Blood* 2009;114:4823–31.
16 Abel AM, Yang C, Thakar MS, *et al*. Natural Killer Cells: Development, Maturation, and Clinical Utilization. *Front Immunol* 2018;9:1869.
17 Paul S, Lal G. The Molecular Mechanism of Natural Killer Cells Function and Its Importance in Cancer Immunotherapy. *Front Immunol* 2017;8:1124.
18 Araujo-Ayala F, Dobaño-López C, Valero JG, *et al*. A novel patient-derived 3D model recapitulates mantle cell lymphoma lymph node signaling, immune profile and in vivo ibrutinib responses. *Leukemia* 2023;37:1311–23.
19 Ai W, Li H, Song N, *et al*. Optimal method to stimulate cytokine production and its use in immunotoxicity assessment. *Int J Environ Res Public Health* 2013;10:3834–42.
20 Riera-Borrull M, Cuevas VD, Alonso B, *et al*. Palmitate Conditions Macrophages for Enhanced Responses toward Inflammatory Stimuli via JNK Activation. *J Immunol* 2017;199:3858–69.
21 Wöbke TK, von Knethen A, Steinhilber D, *et al*. CD69 is a TGF-β/1α,25-dihydroxyvitamin D3 target gene in monocytes. *PLoS One* 2013;8:e64635.
22 Enrich E, Campos E, Martorell L, *et al*. HLA-A, -B, -C, -DRB1, and -DQB1 allele and haplotype frequencies: An analysis of umbilical cord blood units at the Barcelona Cord Blood Bank. *HLA* 2019;94:347–59.
23 Bueno C, Torres-Ruiz R, Velasco-Hernandez T, *et al*. A human genome editing-based MLL::AF4 ALL model recapitulates key cellular and molecular leukemogenic features. *Blood* 2023;142:1752–6.
24 Chiorazzi M, Martinek J, Krasnick B, *et al*. Autologous humanized PDX modeling for immuno-oncology recapitulates features of the human tumor microenvironment. *J Immunother Cancer* 2023;11:e006921.
25 Bonaventura P, Shekarian T, Alcazer V, *et al*. Cold Tumors: A Therapeutic Challenge for Immunotherapy. *Front Immunol* 2019;10:168.